Proceedings of the 3rd Croatian Conference on Earthquake Engineering - 3CroCEE
19–22 March 2025, Split, Croatia

DOI: https://doi.org/10.5592/CO/3CroCEE.2025.112

NUMERICAL EXPERIMENT FOR SHEAR KEY JOINT BEHAVIOUR SIMULATION IN ARCH DAMS: PART 2 – INVESTIGATING THE INFLUENCE OF THE ARCH THICKNESS AND APPLIED FORCE

Violeta Mircevska [(1)], Ana Nanevska [(2)]

[(1)] *Professor, Institute of Earthquake Engineering and Engineering Seismology, University of Ss. Cyril and Methodious, Skopje, R. N. Macedonia., mircevska@iziis.ukim.edu.mk*
[(2)] *Research Assistant, Institute of Earthquake Engineering and Engineering Seismology, University of Ss. Cyril and Methodious, Skopje, R. N. Macedonia., nanevska@iziis.ukim.edu.mk*

Abstract

Nonlinear behavior of contraction joints in arch dams, such as joint opening and sliding caused by hydrostatic pressure and temperature variations, can affect the dam's serviceability. Furthermore, strong seismic events can additionally alter the response in dynamic conditions, impacting the natural period and stress redistribution in the arches and cantilevers. In order to enhance structural integrity with additional shear strength, shear key elements are usually installed along these joints. However, traditional modeling with the actual shear key geometry results in complex analyses. This paper presents a novel approach for simulating shear key behavior by modifying the flat joint concept in ADAD-IZIIS software. The method introduces additional tangential stiffness to the flat joint's stiffness matrix to simulate shear resistance derived from the key geometry. The model uses a uniaxial constitutive law for nonlinear behavior in normal and Coulomb's friction law in the tangential direction. This paper presents the second part of a comprehensive study examining the influence of the arch thickness and applied force through numerical experiments using refined FE models of flat and bevelled shear key joints. The additional shear resistance $F_{\tau,add}$ is calculated by increasing the initial modulus of elasticity $E_{n,\tau}$ in the local shear direction as $E_{n\tau,add}=k_{ad}*E_{n,\tau}$, applying the additional tangential stiffness coefficient k_{ad}, derived from the experimental analyses. Results show that shear resistance is primarily influenced by arch thickness, while the applied force has a lesser effect. In the lower segment, the bevelled shear key increases tangential stiffness by 23% to 27% compared to the flat joint, depending on the applied force. In an upper segment, the same shear key joint exhibits 46% increase, meaning this factor has to be considered in further analysis. The research confirms the efficiency of the proposed approach in simulation of the complex nonlinear behavior of an arch dam constructed with shear key joints.

Keywords: contraction joint, nonlinear behaviour, shear key, numerical experiment

1. Introduction

Arch dams are highly efficient structures that transfer large compressive stresses to the supports through their curved arch geometry, ensuring strength and stability [1]. In order to control tensile stresses development caused by expansion and contraction during concreting, temperature variations, as well as seismic activity, arch dams are constructed in monolithic blocks separated by vertical contraction joints [2]. While these joints enhance construction feasibility, they introduce potential weak points due to imperfections in the grouting process, making them vulnerable to initial damage from temperature variations and strong earthquakes [3]. During a seismic event, relative displacements between monoliths cause joint opening and shear sliding, significantly redistributing internal forces both during and after the seismic event due to residual joint openness. Previous research [4][5][6][7][8] has shown that the nonlinear behavior of these joints, including their opening and shear sliding, increases the natural period of the dam and leads to a significant redistribution of stresses in the arches and cantilevers. This emphasizes the importance of accurate numerical simulation of contraction joint behaviour for evaluating the static and seismic stability of arch dams.

To improve the compactness, shear strength and enhance the overall integrity of arch dams, shear key elements are often incorporated along the joints in the radial and/or longitudinal directions. These elements improve monolithic integrity and provide additional shear resistance especially in thinner

DOI: https://doi.org/10.5592/CO/3CroCEE.2025.112

dams, by resisting normal displacements caused by joint opening [9]. However, their analytical modeling remains complex due to challenges in representing their specific geometry, as well as proper modeling of the interaction effects between opening and sliding in the joints.

The first part of this study titled "*Numerical experiment for shear key joint behaviour simulation in arch dams: Part 1 – Investigating the influence of the key shape and angle*", focused on the numerical simulation of shear key joint behavior, specifically investigating the influence of shear key shape and angle. Part 1 also provided a comprehensive review of the existing literature on the subject, discussing the development and application of various numerical models for simulating the nonlinear behavior of construction joints in arch dams. To avoid redundancy, this literature review will not be reiterated here; however, readers are encouraged to refer to Part 1 for a review of the state-of-the-art research and background on the topic.

This second part of the study builds on the findings, established methodology and nonlinear constitutive model for simulating shear key joint behavior developed in Part 1. This part of the study further expands the investigation to explore the effects of additional critical parameters, such as arch thickness and applied force on the shear key joint behavior. Additional numerical experiments are conducted using the same constitutive model and the 3D flat joint contact element previously implemented in the ADAD-IZIIS software [10]. By analysing additional parameters, the study offers a deeper exploration of the mechanical behavior of shear key joints and provides valuable insights into their performance under varying loading and geometric conditions. Together, these two parts establish a robust and comprehensive framework for assessing the static and seismic stability of arch dams with shear key joints, contributing valuable insights to both research and practical engineering applications.

2. 3D flat contact element implemented in the ADAD-IZIIS software

The modeling approach is based on the 3D flat contact element previously integrated into the ADAD-IZIIS software [10], as described in Part 1. A schematic representation of this contact element is provided in Fig. 1, illustrating the contact surfaces that represent the two faces of two different finite elements in the contact, defined by eight points each.

This contact element simulates the nonlinear behavior of flat joints by capturing coupled effects in all three directions of the contact. The nonlinear behaviour in the normal direction is governed by follows a uniaxial constitutive law (Fig. 2a),while the tangential behavior adheres to the Coulomb's law of friction in both tangential directions (Fig. 2b). The mechanical properties of the grouting joint material are slightly lower than those of the concrete in the monoliths, with nonlinear behaviour modelled in the joints and linear behaviour in the monoliths. Readers are referred to Part 1 for a detailed description of the material properties.

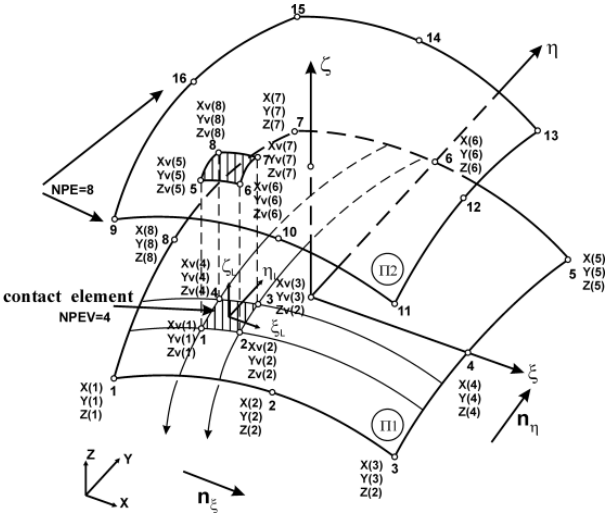

Figure 1. Schematic representation of the 8-point contact element

DOI: https://doi.org/10.5592/CO/3CroCEE.2025.112

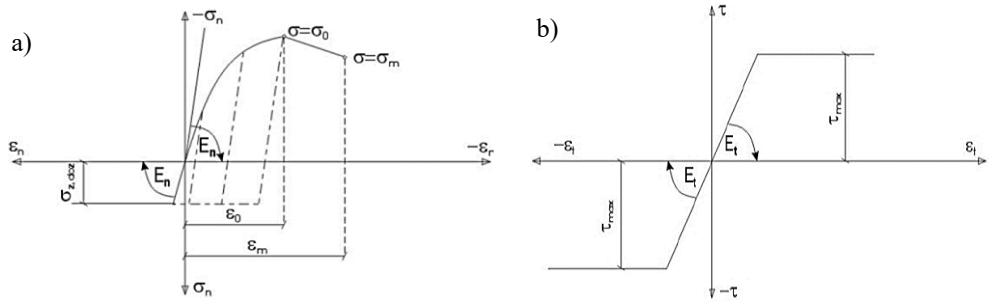

Figure 2. Constitutive relations for the behaviour of the grouting mass in construction joints in the a) normal direction and b) two tangential directions

3. Numerical experiment for shear key joint behaviour simulation in arch dams

The numerical experiment builds upon the same foundational approach and assumptions established in Part 1 of the study, with modifications to the flat element concept in the tangential direction by introducing an additional tangential stiffness induced by the geometric shear resistance of the shear key element. The tangential shear resistance is modelled as:

$$F\tau = F\tau_f + Fc + F\tau_{ad} = (\mu\sigma_n + c) + F\tau_{ad} \quad (1)$$

where $F\tau_{ad}$ represents the additional shear resistance obtained by increasing the initial modulus of elasticity ($E_{1,\tau}$) in the direction of the shear key element, as described by:

$$E_{1\,\tau,add} = k_{ad} * E_{1,\tau} \quad (2)$$

Here, k_{ad} is the coefficient of additional tangential stiffness, determined through numerical experiments. In this part of the study, different numerical experiments are conducted to investigate the impact of arch thickness. The finite element models are adopted with smaller thickness (140 cm) to represent a segment in the higher part of the dam. One model has the flat joint configuration (Model 4, Fig. 3a) while the other two have are with the bevelled shear key joint (Model 5, Fig. 3b) and unbevelled shear key joint (Model 6, Fig. 3c).

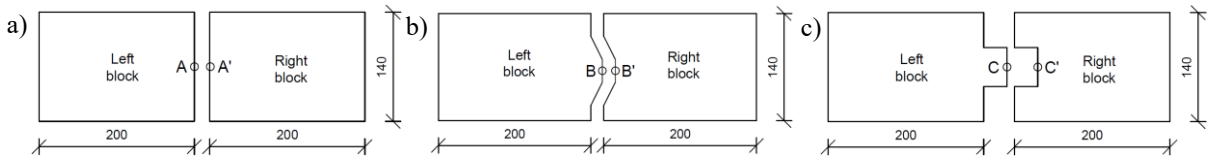

Figure 3. Geometric characteristics: a) Model 4, b) Model 5, and c) Model 6

The finite element meshes and boundary conditions for these models are presented in Fig. 4 and follow the same setup as in Part 1, ensuring consistency in the numerical experiments. For all models, the left side is fixed, and a horizontal static force is applied at the end (not shown in the figures) and along the contact, simulating both bending and shearing force, respectively. The static force is incremented according to $F_{fmi} = F_s * f_{mi}$, where the multiplier f_{mi} ranges from 1 to 50 and the experiment continues until the uniaxial compressive strength in the contact's normal direction is reached. Models 5 and 6 use a constant tangential modulus of elasticity, while for Model 4 various coefficients k_{ad} are employed until the contact shear sliding values between the flat joint and shear key joints coincide.

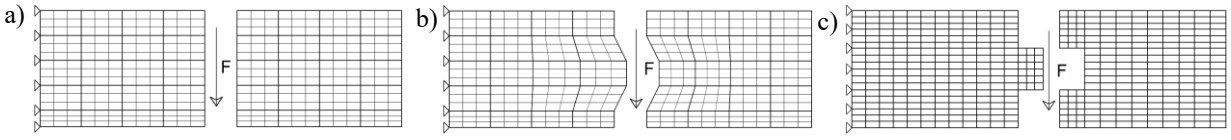

Figure 4. Finite element mesh and boundary conditions for: a) Model 4, b) Model 5 and c) Model 6

Proceedings of the 3rd Croatian Conference on Earthquake Engineering - 3CroCEE
19–22 March 2025, Split, Croatia

DOI: https://doi.org/10.5592/CO/3CroCEE.2025.112

4. Results from numerical experiments

The numerical experiments conducted in the second part of the study provide an in-depth evaluation of the behaviour of shear key joints with a particular emphasis on the influence of arch thickness and applied forces. Separate analyses are performed for both bevelled and unbevelled shear key joints, with comparisons made against the flat joint with various adopted coefficients k_{ad}. For the bevelled shear key joint (Model 5), comparisons with the flat joint model (Model 4) were made for k_{ad} values of k_{ad}=1.0 (equal tangential stiffness for both models), k_{ad}=1.15, k_{ad}=1.30 and k_{ad}=1.46. For the unbevelled shear key joint (Model 6), k_{ad} values of k_{ad}=1.0, k_{ad}=1.30, k_{ad}=1.46 and k_{ad}=1.86 were employed in Model 4 for comparative analysis. The results presented are derived from the analysis conducted under a pure shear force acting along the length of the contact.

The horizontal displacements of the monolithic block in both directions for an incremental load factor of f_{mi}=50 are presented in Fig. 5 for: a) Model 4 with k_{ad}=1.0, b) Model 5 and c) Model 6. Fig. 6 highlights the zones of open contact elements across all joints for the same load factor. The spatial distribution of open contact elements is along the contact, which is consistent with the acting shearing force. The percentage differences underscore reduced openings in the unbevelled shear key joint compared to the similar values in the bevelled and flat joint models.

Fig. 7 presents the stress-strain relationships in critical contact elements in which extreme responses, such as maximum opening and shear sliding are observed. The figures shows the stress-strain relationships for: Model 4 with k_{ad}=1.0 in the contact elements in which the maximum: a) opening in the direction of the normal (CE 25) and b) sliding in the direction of the shear key element (CE 154) occur; Model 5 in the contact elements in which the same extremes occur in the corresponding elements: c) CE 25 and d) CE 154 and Model 6 in the contact elements where the extremes occur: e) CE 25 and f) CE 77. The position of these contact is illustrated in each subfigure and highlights the localized responses unique for each joint configuration.

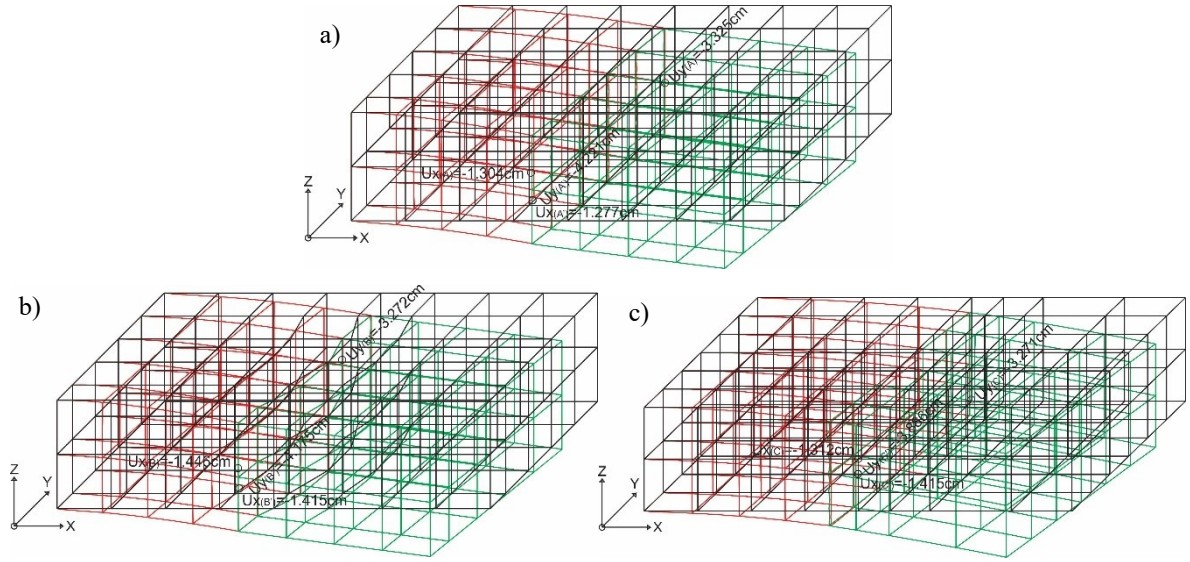

Figure 5. Horizontal displacements in the monoliths in both global directions (f_{mi}=50): a) Model 4 with k_{ad}=1.0, b) Model 5 and c) Model 6

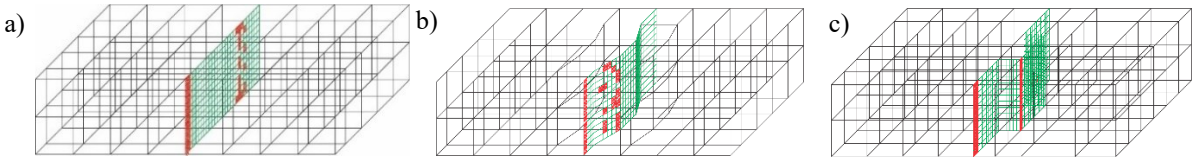

Figure 6. Open contact elements (f_{mi}=50): a) Model 4 with k_{ad}=1.0 (18% open elements), b) Model 5 (18% open elements) and c) Model 6 (17% open elements)

DOI: https://doi.org/10.5592/CO/3CroCEE.2025.112

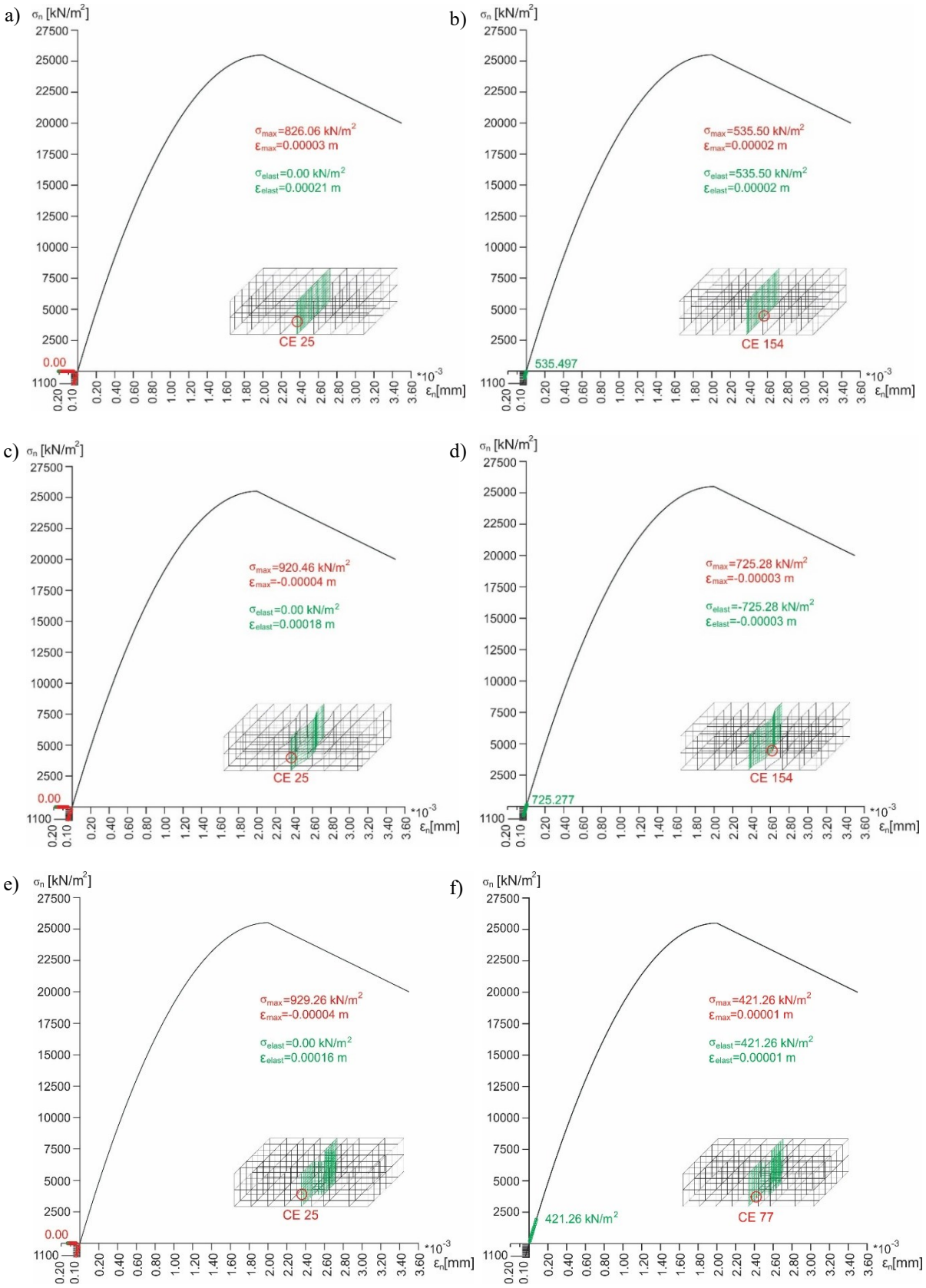

Figure 7. Normal stress–strain relationship (f_{mi}=50): Model 4 (k_{ad} =1.0) for elements with maximum: a) opening in the direction of the normal (CE 25), b) sliding in the direction of the element (CE 154); Model 5: c) opening (CE 25), d) sliding (CE 154); and Model 6: e) opening (CE 25) and f) sliding (CE 77)

Proceedings of the 3rd Croatian Conference on Earthquake Engineering - 3CroCEE
19–22 March 2025, Split, Croatia

DOI: https://doi.org/10.5592/CO/3CroCEE.2025.112

For these analysed upper dam segments, Fig. 8 to Fig. 11 illustrate the histories of extremes of key parameters, including shear sliding deformations, contact openings, and horizontal displacements in the y-direction for both the left and right blocks. These parameters are calculated as a function of the incremental load factor across Models 5 and 6, and Model 4 with all of the calculated coefficients of additional tangential stiffness k_{ad}.

The most pronounced differences between the two models that are compared are observed in sliding deformations when all models have the same modulus of elasticity (k_{ad}=1.0), as shown in Fig. 8. Under a loading factor of f_{mi}=50, the flat joint (Model 4 with kad=1.0) exhibits a maximum shear sliding of γ_{max}=1.35 mm, whereas the bevelled shear key joint (Model 5) reduces the deformation by 44% with a maximum value of γ_{max}=0.76 mm. The unbevelled shear key joint model (Model 6) demonstrates even greater resistance, with a 68% reduction of shear sliding compared to the flat joint, with maximum value of γ_{max}=0.43 mm. As the coefficient k_{ad} increases, the sliding deformation in the flat joint approaches that of shear key joints. Good agreement is achieved for k_{ad}=1.46 between the sliding values of flat and bevelled shear key joint, while for the unbevelled and flat joint the sliding values are equal for k_{ad}=1.85. These values represent the resistance effects of the different shear key types in the upper dam segments. The shear sliding extremes are concentrated near the middle to lower part of the contact zone for all models (Figure 7b, d, f).

Consistent with the applied shear force, sliding dominates over the contact openings across all analysed models. Maximum openings occur at the lower edge of the contact zone (Figure 7a, c, d) in contact element CE 25 for all of the models. For all loading factors, the bevelled shear key joint (Model 5) shows smaller maximum contact openings, δ_{max}=0.179 mm, compared to the flat joint (Model 4), δ_{max}=0.213 mm, even with increased tangential stiffness (Fig. 9 a). Similarly, the unbevelled shear key joint (Model 6), exhibits maximum openings δ_{max}=0.165 mm, much smaller than those in flat joint (Model 4), even for various values of k_{ad} and increased tangential stiffness, Fig 9b.

Horizontal displacements in the monolithic blocks exhibit larger differences when models have equal tangential stiffness, with differences decreasing as k_{ad} increases. While the displacements of the flat joint approach those of the shear key joints, they do not fully converge. The left monolithic block, constrained by boundary conditions shows smaller maximum displacements than the right block (Fig. 11 and 12). In the bevelled shear key joint (Model 5), maximum displacements are u_y=41.75 mm in the right (Fig. 12a) and u_y=32.72 mm in the left block (Fig 11.a). These displacements are both larger than the corresponding values in the flat joint (Model 4 with k_{ad}=1.0), with values u_y=44.36 mm in the right and u_y=35.80 mm in the left block. For the unbevelled shear key joint (Model 6), the maximum displacement are u_y=44.36 mm in the right (Fig. 12b) and u_y=36.68 mm in the left block (Fig. 11b). All of these displacements are notably higher than those observed in the joints of the lower dam segment (Part 1 of the study). The reduction in relative displacements is greater in the unbevelled shear key joint compared to the bevelled shear key joint, which is consistent with its superior sliding resistance behavior shown in earlier results.

Based on the results of the numerical experiments and their comparison with lower dam segment results, a linear interpolation was performed to determine the k_{ad} values needed for increasing the tangential modulus of elasticity $E_{1,t}$ for both shear key types as a function of arch cantilever thickness (Fig. 12). This approach allows straightforward calculation of the additional tangential stiffness for joints of each shear key type across varying dam cantilever thicknesses that will be applied to different segments along the dam height. The calculated stiffness values are integrated into the contact element stiffness matrix, ensuring necessary adjustments in the numerical model.

DOI: https://doi.org/10.5592/CO/3CroCEE.2025.112

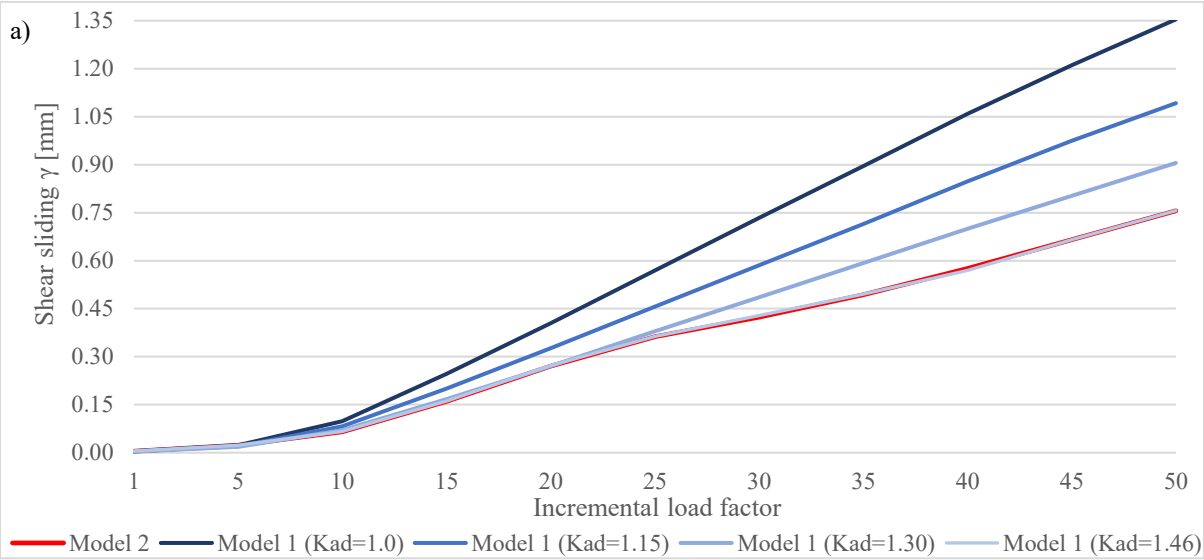

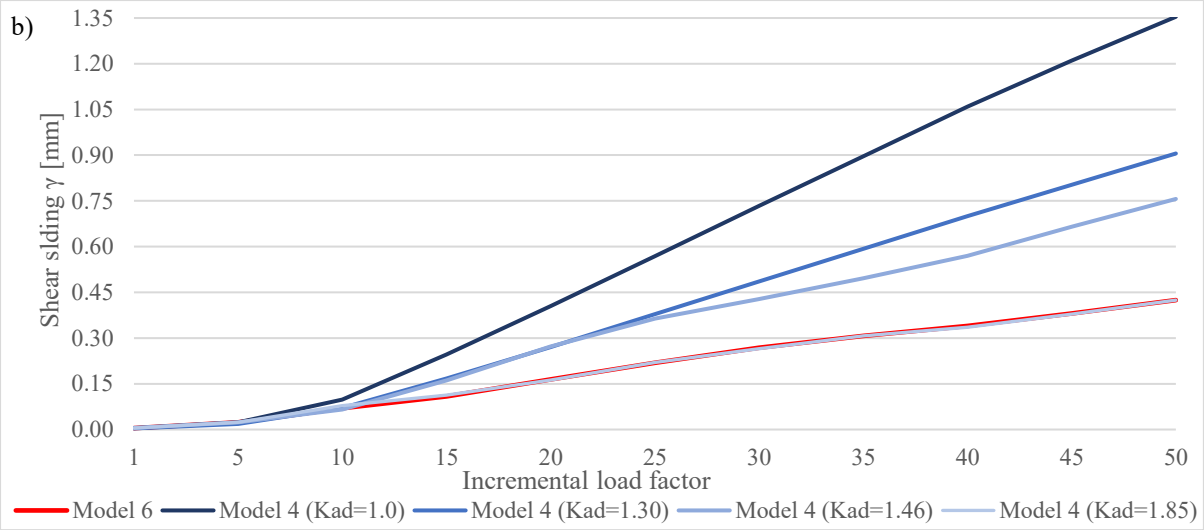

Figure 8. History of maximum shear sliding in the contact as a function of the incremental load factor for: (a) Model 1 and Model 2, (b) Model 1 and Model 3

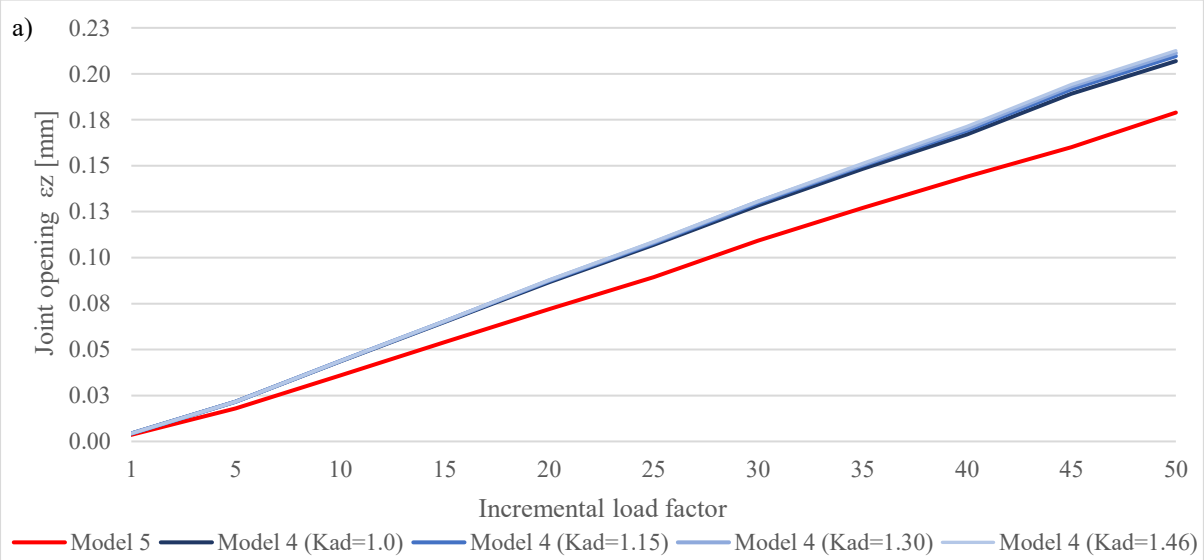

Proceedings of the 3rd Croatian Conference on Earthquake Engineering - 3CroCEE
19–22 March 2025, Split, Croatia

DOI: https://doi.org/10.5592/CO/3CroCEE.2025.112

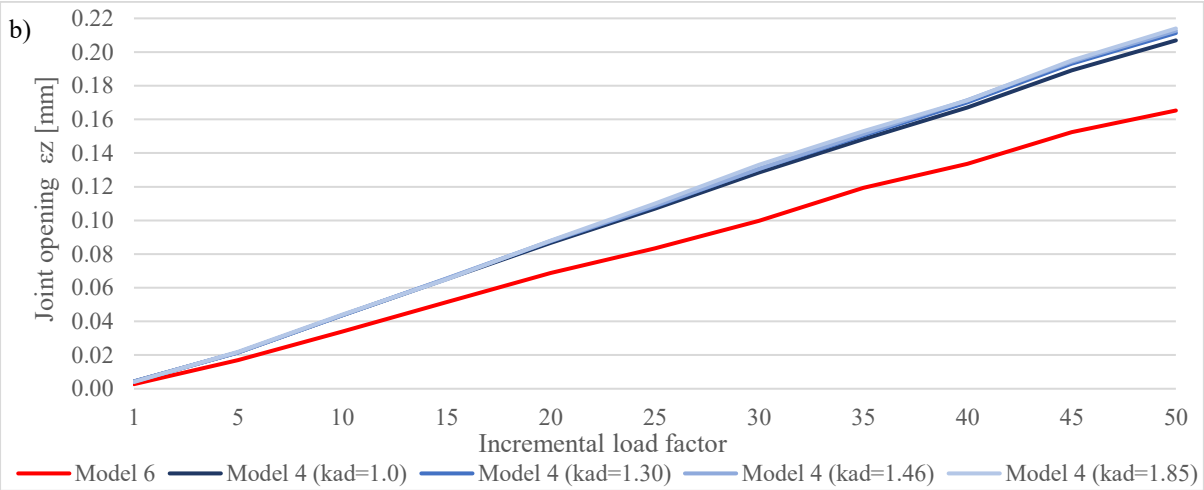

Figure 9. History of maximum opening in the contact as a function of the incremental load factor for: (a) Model 1 and Model 2 and (b) Model 1 and Model 3

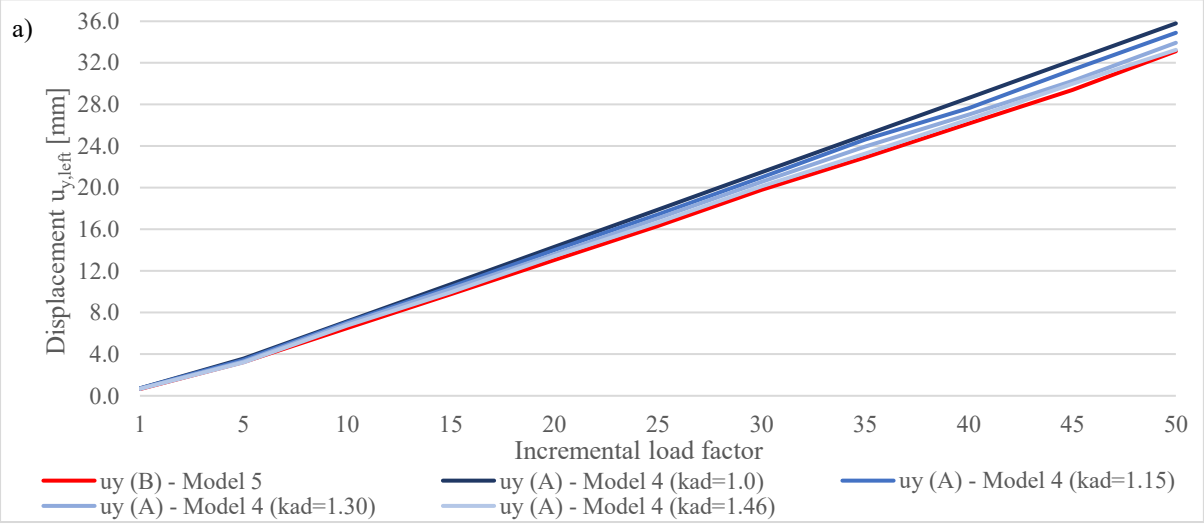

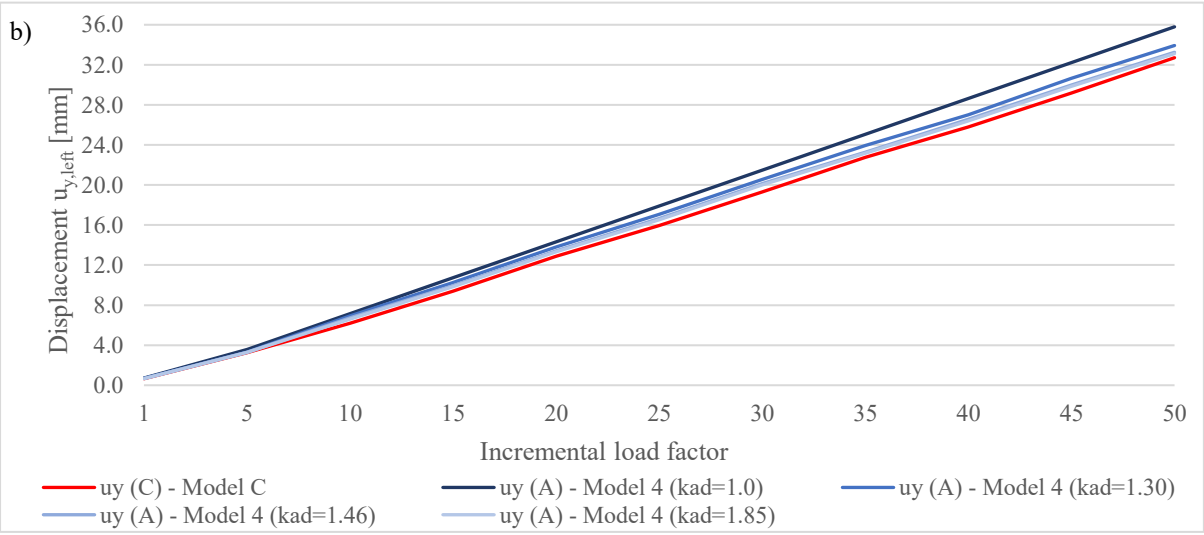

Figure 10. History of maximum horizontal displacements in the global y-direction in the left monolithic block as a function of the incremental load factor for: (a) Model 1 and Model 2 and (b) Model 1 and Model 3

DOI: https://doi.org/10.5592/CO/3CroCEE.2025.112

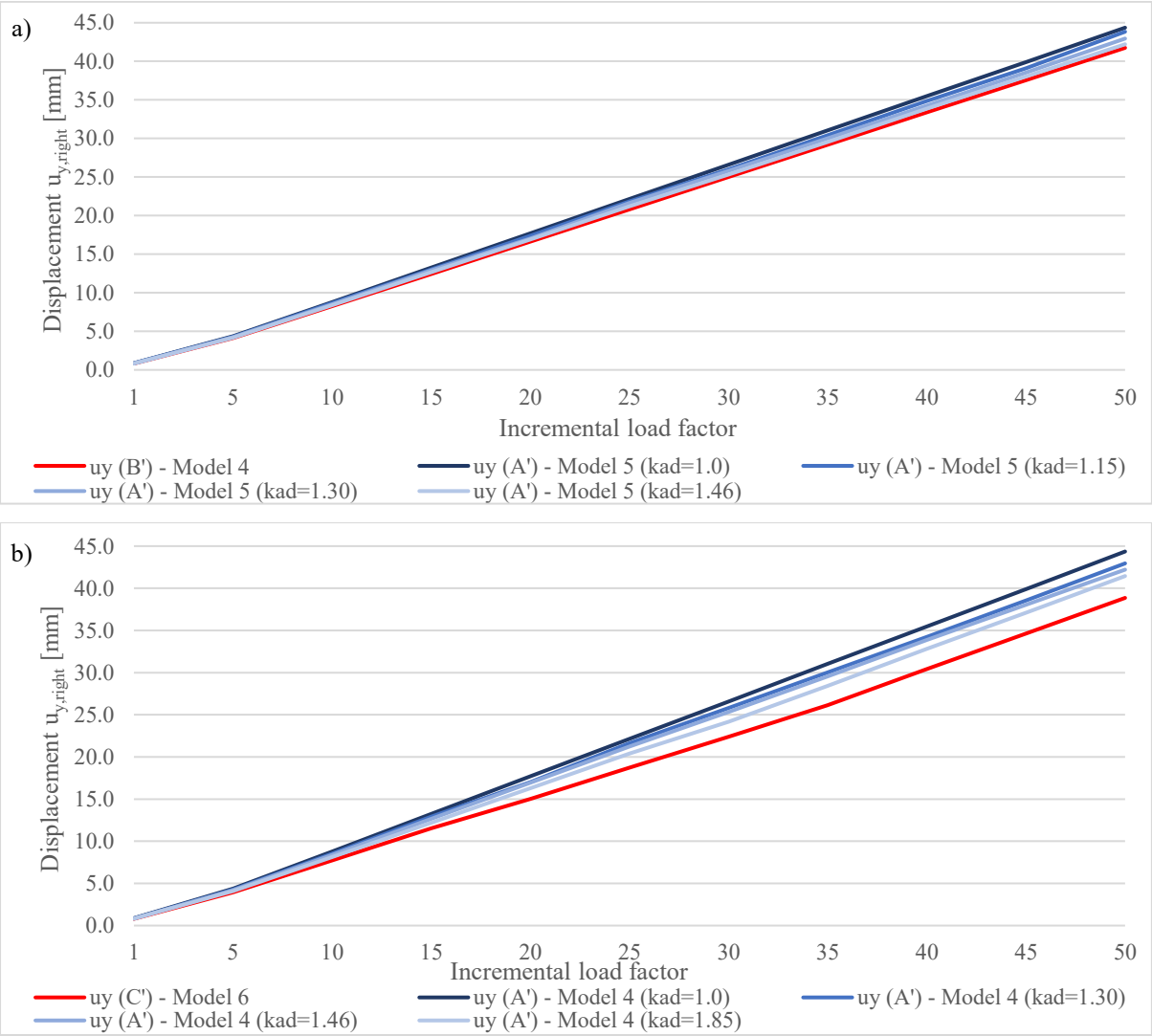

Figure 11. History of maximum horizontal displacements in the global y-direction in the right monolithic block as a function of the incremental load factor for: (a) Model 1 and Model 2 and (b) Model 1 and Model 3

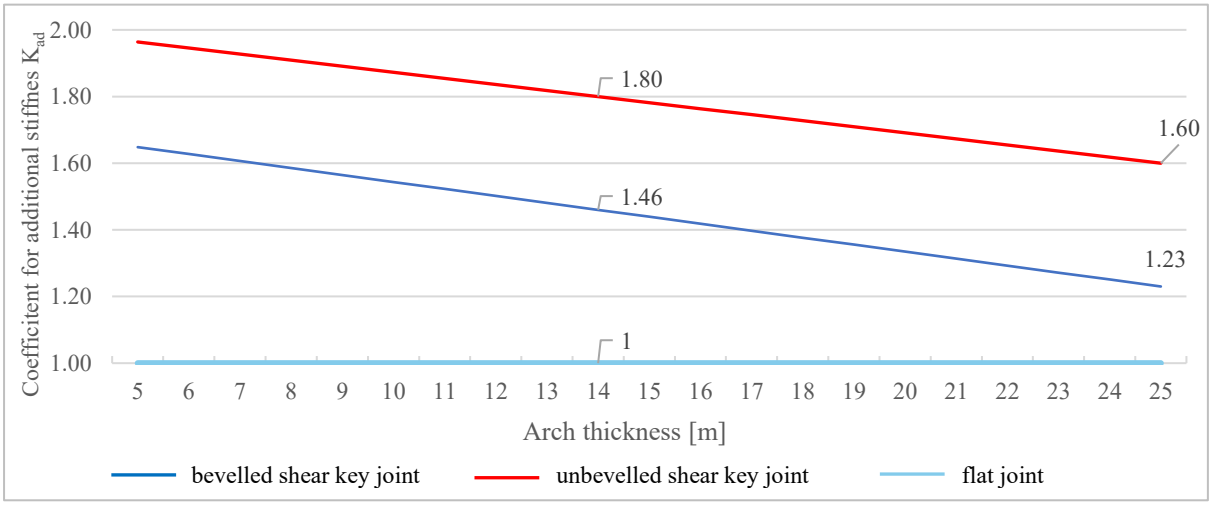

Figure 12. Calculation of the coefficient for additional tangential stiffness k_{ad} needed for increase of the tangential modulus of elasticity $E_{1,t}$ as a function of the arch thickness

Proceedings of the 3rd Croatian Conference on Earthquake Engineering - 3CroCEE
19–22 March 2025, Split, Croatia

DOI: https://doi.org/10.5592/CO/3CroCEE.2025.112

The same models in the lower dam segment from Part 1 of the study (Models 1, 2, and 3) are analysed again, this time to examine the effects of a shearing force. Fig. 13 presents the histories of maximum sliding deformations for Models 2 and 3, compared to Model 1 under varying adopted values for k_{ad}. For the unbevelled shear key joint (Model 3), sliding deformations in the lower dam segment under a sliding force are reduced by 50%, with γ_{max}=0.68 mm, compared to the flat joint (Model 1 with k_{ad}=1.0), where γ_{max}=1.40 mm (Fig. 13b). This reduction is consistent regardless of whether the applied force is bending or shear force. For the bevelled shear key joint (Model 2), the reduction under a shearing force is smaller compared to Model 3, showing a 30% decrease in sliding deformation, γ_{max}=0.96 mm compared to the flat joint, γ_{max}=1.40 mm (Model 1 with k_{ad}=1.0), as shown in Fig. 13a. Under bending force, as examined in Part 1 of the study, the shear sliding reduction in the bevelled shear key joint is approximately 25%. Comparing these findings with the bending force results from Part 1 confirms that the type of applied force has minimal to no impact on the additional tangential stiffness needed to model shear key joints effectively.

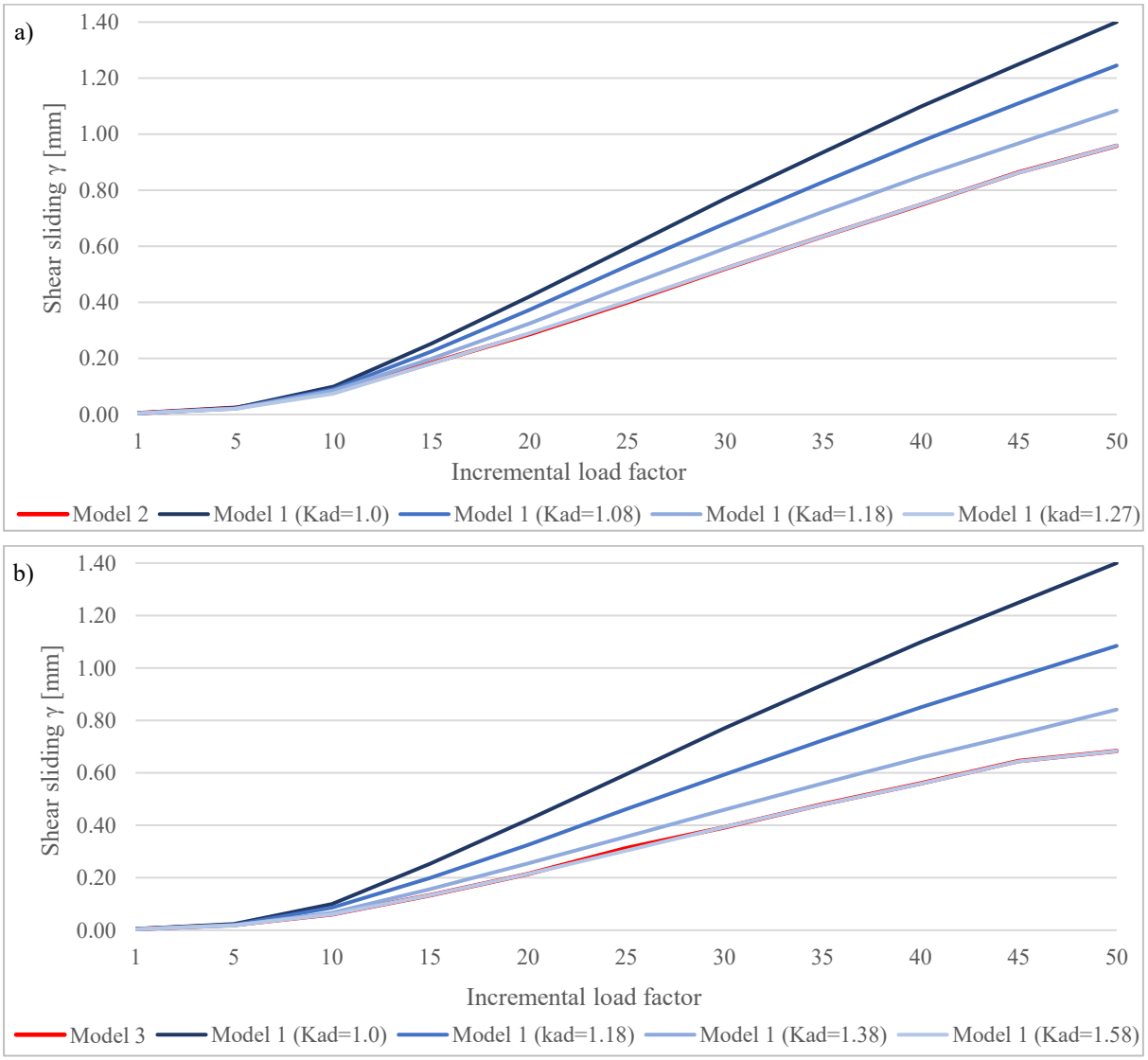

Figure 13. History of maximum shear sliding in the contact as a function of the incremental load factor for shearing force acting along the contact: (a) Model 1 and Model 2, (b) Model 1 and Model 3

Proceedings of the 3rd Croatian Conference on Earthquake Engineering - 3CroCEE
19–22 March 2025, Split, Croatia

DOI: https://doi.org/10.5592/CO/3CroCEE.2025.112

5. Discussion of the results and conclusions

The aim of this research is to quantify the additional tangential stiffness representing the shear resistance of shear key joint elements with various geometries. The main focus is to derive these tangential stiffness values that can be applied to flat joints, thereby eliminating the need for detailed geometric modeling to capture the complexity of shear key joint geometry and behavior. These computed values, expressed as additional tangential stiffness coefficient are integrated into the flat joint contact elements' stiffness matrix, modifying the constitutive law to accurately simulate nonlinear behavior of the joint in the direction of the shear key elements, which may be implemented in one or two directions. The second part of the study focuses on investigating the influence of arch thickness and applied force.

The most pronounced differences among the analysed parameters are observed in the sliding shear deformations at the contact. The tangential stiffness coefficient k_{ad} is determined by equating the sliding deformations of the flat joint to those of the shear key joints. In the upper dam segments, the bevelled shear key shows a 46% increase in tangential stiffness, compared to 27% in the lower parts. The unbevelled shear key exhibits a 70% increase, emphasizing the impact of arch thickness. These results affirm that the segment thickness directly influences tangential stiffness, with each joint configuration contributing differently to the resistance in tangential direction. In both parts of the study, it is confirmed that the tangential stiffness increase varies depending on the type of shear key, with unbevelled joints consistently showing greater stiffness increase than bevelled joints. Furthermore, Part 2 confirms that arch thickness significantly affects shear key behavior, even for the same joint configuration.

In the upper segments under shear force, both shear key joint types of exhibits reduced joint openings compared to the flat joint, with differences that do not diminish with the increase of tangential stiffness. However, these differences remain relatively small, around 0.034 mm for the bevelled and 0.049 mm for the unbevelled shear key joint. It can be concluded that despite variations in sliding deformations, joint openings are exhibit similar values across all modes. Regarding open element zones, the unbevelled shear key joint shows fewer open elements, concentrated on the key element within a small area near the contact's end. In contrast, the bevelled shear key joint displays open elements in both upper and lower key regions, with more pronounced openings in the lower section, aligning with the maximum observed openings in that area. Maximum horizontal displacements in the global y-direction, as well as relative displacements between the monolithic blocks, closely correspond to the observed shear sliding behavior. Arch thickness significantly influences these displacements, with larger values observed in the thinner upper sections compared to the thicker lower section of the dam, which is expected. Additionally, the response curves for all joint types demonstrate strong consistency across the analysed parameters for all types of joints.

The study findings confirm that the favourable shear key joint geometry (of both analysed types) significantly increases the tangential stiffness compared to flat joints. The key factors influencing shear resistance include not only the geometry of the joints (shape and angle of the key element), but also the arch segment's thickness, and, to a lesser extent, the type of applied force. Notably, the segment's thickness plays a critical role even for joints with identical shear key configurations, highlighting the need to account for this parameter in further analyses.

The research confirms the efficiency of the proposed approach in simulation of the complex nonlinear behavior of an arch dam constructed with shear key joints, eliminating the need for explicit geometric modeling. The model will be applied to simulate contraction joints in an arch dam, evaluating the impact of the different joint types on stress redistribution and the overall structural response under static and dynamic loading conditions.

DOI: https://doi.org/10.5592/CO/3CroCEE.2025.112

References

[1] Talatahari, S., Salami M., Parsiavash, R. (2016): Optimum design of double curvature arc dams using a quick hybrid charged system search algorithm. *Iran University of Science & Technology*, **6**, 227-243, Corpus ID: 53392743.

[2] Du, C. B., Jiang, S. Y. (2010): Effects of contraction joints and key slots on the seismic responses of arch dam (in Chinese). *Journal of Hydroelectric Engineering*, **29** (5), 1–5.

[3] Ahmadi, M. T., Izadinia, M., Bachmann, H. (2001): A discrete crack joint model for nonlinear dynamic analysis of concrete arch dam. *Computers and Structures,* **79** (4), 403-420, https://doi.org/10.1016/S0045-7949(00)00148-6.

[4] Fenves, G. L., Mojtahedi, S., Reimer, R. B. (1992): Effect of contraction joints on earthquake response of an arch dam. *Journal of Structural Engineering*, **118** (4), 1039—1055, https://doi.org/10.1061/(ASCE)0733-9445(1992)118:4(1039).

[5] Lau, D. T., Noruziaan, B., Razaqpur, A. G. (1998): Modelling of contraction joint and shear sliding effects on earthquake response of arch dams. *Earthquake Engineering and Structural Dynamics*, **27**, 1013-1029, https://doi.org/10.1002/(SICI)1096-9845(199810)27:10<1013::AID-EQE765>3.0.CO;2-0.

[6] Tzenkov, A. D., Lau, D. T. (2002): Seismic analysis of concrete arch dams with contraction joints and non-linear material models, *7th U.S. National Conference on Earthquake Engineering*, Boston, Massachusetts.

[7] Toyoda, Y., Ueda M., Shiojiri, H. (2002): Study of joint opening effects on the dynamic response of an existing arch dam, *15th ASCE Engineering Mechanics Conference*, Columbia University, New York.

[8] Noble, C. R., Solberg J. (2004): Nonlinear seismic analysis of Morrow Point dam. *A Study for the United States Bureau of Reclamation*, UCRL-TR-202545.

[9] Guerra, A. (2007): Shear key research project – Literature review and finite element analysis. Dam Safety Technology Development Program, U.S. Department of the Interior, Bureau of Reclamation, *Report DSO-07-05*.

[10] ADAD-IZIIS – Software for analysis and design of arch dams. *Institute of Earthquake Engineering and Engineering Seismology*, University of Ss. Cyril and Methodious, Skopje, R. N. Macedonia.